

Viscoelastic properties of human mesenchymally-derived stem cells and primary osteoblasts, chondrocytes, and adipocytes

Eric M. Darling^{a,b}, Matthew Topel^b, Stefan Zauscher^c,
Thomas P. Vail^{a,1}, Farshid Guilak^{a,b,c,*}

^aDepartment of Surgery, Duke University Medical Center Durham, NC 27710 USA

^bBiomedical Engineering, Duke University Medical Center Durham, NC 27710 USA

^cMechanical Engineering and Materials Science, Duke University Medical Center Durham, NC 27710 USA

Accepted 25 June 2007

Abstract

The mechanical properties of single cells play important roles in regulating cell-matrix interactions, potentially influencing the process of mechanotransduction. Recent studies also suggest that cellular mechanical properties may provide novel biological markers, or “biomarkers,” of cell phenotype, reflecting specific changes that occur with disease, differentiation, or cellular transformation. Of particular interest in recent years has been the identification of such biomarkers that can be used to determine specific phenotypic characteristics of stem cells that separate them from primary, differentiated cells. The goal of this study was to determine the elastic and viscoelastic properties of three primary cell types of mesenchymal lineage (chondrocytes, osteoblasts, and adipocytes) and to test the hypothesis that primary differentiated cells exhibit distinct mechanical properties compared to adult stem cells (adipose-derived or bone marrow-derived mesenchymal stem cells). In an adherent, spread configuration, chondrocytes, osteoblasts, and adipocytes all exhibited significantly different mechanical properties, with osteoblasts being stiffer than chondrocytes and both being stiffer than adipocytes. Adipose-derived and mesenchymal stem cells exhibited similar properties to each other, but were mechanically distinct from primary cells, particularly when comparing a ratio of elastic to relaxed moduli. These findings will help more accurately model the cellular mechanical environment in mesenchymal tissues, which could assist in describing injury thresholds and disease progression or even determining the influence of mechanical loading for tissue engineering efforts. Furthermore, the identification of mechanical properties distinct to stem cells could result in more successful sorting procedures to enrich multipotent progenitor cell populations.

© 2007 Elsevier Ltd. All rights reserved.

Keywords: Cell mechanics; Atomic force microscopy; Osteoblast; Chondrocyte; Adipocyte; ADAS cell; MSC; Mechanotransduction

1. Introduction

The viscoelastic properties and deformation behavior of cells play important roles in many biophysical and biological responses (see reviews in Costa, 2003; Guilak, 2000; Huang et al., 2004; Ingber, 2003; Zhu et al., 2000).

For example, the mechanical properties of cells can affect their physical interactions with the surrounding extracellular matrix (Alexopoulos et al., 2005; Guilak and Mow, 2000b), potentially influencing the process of mechanical signal transduction in mesenchymal tissues (Buckwalter et al., 2006; Burkholder, 2007; Guilak et al., 1997; Ingber, 2006; Liedert et al., 2006; Robling et al., 2006; Setton and Chen, 2004). Furthermore, alterations in cell properties have been shown to reflect specific phenotypes associated with cellular subpopulations (Darling et al., 2006), disease (Trickey et al., 2000) or malignant transformation (Darling et al., 2007; Guck et al., 2005; Thoumine and Ott, 1997). Of recent interest has been the identification of novel

*Corresponding author: Orthopaedic Research Laboratories, 375 MSRB, Box 3093, Duke University Medical Center, Durham, NC 27710, USA. Tel.: +1 919 684 2521; fax: +1 919 681-8490.

E-mail address: guilak@duke.edu (F. Guilak).

¹Current address: Department of Orthopaedic Surgery, University of California, San Francisco, Box 0728, 500 Parnassus Avenue, MU326W, San Francisco, CA 94143-0728 USA.

Nomenclature			
μ	apparent viscosity	E_0	instantaneous modulus
E_{elastic}	elastic modulus (from Hertz model)	E_R	relaxed modulus
E_{equil}	equilibrium modulus (from Hertz model at equilibrium)	τ_σ	time of relaxation of deformation under constant load
		τ_ε	time of relaxation of load under constant deformation

biological markers, or “biomarkers,” that can be used as surrogate measures of cell phenotype in different states of disease, transformation, or differentiation.

The viscoelastic mechanical properties of single cells have been quantified using a variety of testing methods, including micropipette aspiration, cytoindentation, magnetic bead rheometry, optical traps, and atomic force microscopy (AFM) (e.g., Bausch et al., 1998; Charras and Horton, 2002a; Evans and Yeung, 1989; Guck et al., 2005; Hochmuth, 2000; Mahaffy et al., 2004; Shin and Athanasiou, 1999; Yourek et al., 2007). Differences in the assumptions and constitutive models used in developing these testing methods and differences in cell sources, however, make a direct, quantitative comparison across studies currently infeasible.

The goals of this study were: (i) to test whether the elastic and viscoelastic properties of primary mesenchymally-derived cells (i.e., chondrocytes, osteoblasts, and adipocytes) indicate cell phenotype and (ii) to test whether undifferentiated stem cells of mesenchymal origin exhibit distinct biomechanical properties compared to primary differentiated cells. Mechanical properties were determined in either rounded or flattened morphologies for primary, adult cells harvested from articular cartilage, bone, or adipose tissue, as well as two sources of stem cells: adipose-derived adult stem (ADAS) cells (Gimble and Guilak, 2003; Guilak et al., 2006) and bone marrow-derived adult mesenchymal stem cells (MSCs) (Caplan, 1991; Jiang et al., 2002).

2. Materials and method

2.1. Cell harvest and culture conditions

2.1.1. Chondrocytes

Chondrocytes were isolated from full thickness articular cartilage from human femoral heads, harvested during joint replacement surgery ($n = 46$ spherical, $n = 50$ spread cells from five donors, ages: 34–47 years). Only macroscopically normal regions of cartilage were used. Cells were isolated by sequential digestion with pronase (1% wt/vol, 1 h, Calbiochem, San Diego, CA) and collagenase (0.4% wt/vol, 2 h, Worthington, Lakewood, NJ) (Kuettner et al., 1982). Cells were suspended in culture media, consisting of high glucose DMEM (Gibco, Carlsbad, CA), 1x penicillin/streptomycin (Gibco), and 10% FBS (Gibco) and seeded onto poly-L-lysine (PLL)-coated polystyrene, 35 mm Petri dishes (Becton Dickinson, Bedford, MA). Biomechanical testing was performed at room temperature at 1 h and after 1–4 days.

2.1.2. Osteoblasts

Osteoblasts were isolated from human femoral heads harvested at the time of joint replacement surgery ($n = 43$ spherical, $n = 43$ spread cells

from five donors, ages: 39–69 years). Primary cells were isolated from the bone using previously established techniques (Fermor et al., 1998; Gundle and Beresford, 1995; Ng et al., 2005). Briefly, bone trabeculae were removed from the femoral head and washed vigorously to remove blood and marrow, then centrifuged. The supernatant was removed, and the tissue was washed again. Finally, bone trabecular fragments were placed on tissue-culture treated Petri dishes, fed with culture media containing 10 nM dexamethasone (Sigma) and 100 μ M ascorbate-2-phosphate (Sigma) for 2 weeks to allow primary osteoblasts to migrate from the bone to the surface of the Petri dish (Gundle et al., 1995). The cells were removed from the surface using 0.05% Trypsin/EDTA (Gibco) and seeded onto PLL-coated Petri dishes. Primary osteoblasts were tested in culture media at room temperature at 1 h and 1 day.

2.1.3. Adipocytes

Adipocytes were isolated from fat pads harvested at the time of joint replacement surgery ($n = 48$ cells from five donors, ages: 55–75 years). Mature cells were isolated from the tissue using established techniques (Ferynhough et al., 2004; Zhang et al., 2000). Briefly, tissue from the fat pad was diced in phosphate buffered saline (PBS, Gibco), washed several times, and centrifuged at $50 \times g$ for 5 m. The tissue was then digested with 0.1% type I collagenase for 1 h at 37°C. The resulting fluid was filtered through 1-mm nylon mesh and washed three times with PBS before being re-suspended in culture media. The isolated adipocytes were then placed in SlideFlasks (Nalge Nunc International, Rochester, NY) filled with culture media and cultured inverted for 1 week. Because adipocytes attached to surfaces slowly, only one time point was used to evaluate cell mechanics (1 week). Data associated with this time point were used for comparison in both the spherical and spread morphology analyses.

2.1.4. ADAS cells

Human ADAS cells were obtained from liposuction waste of subcutaneous abdominal adipose tissue from non-smoking, non-diabetic female donors ($n = 55$ spherical, $n = 52$ spread cells from 3 donors, ages: 34–47 years, Zen-Bio, Inc., Durham, NC). Cells were grown to passage 4 (P4) in expansion media consisting of DMEM/F12 (Cambrex Bio Science, Walkersville, MD), 10% FBS, 1% penicillin–streptomycin–fungizone, 0.25 ng/ml transforming growth factor- β 1 (R&D Systems, Minneapolis, MN), 5 ng/ml epidermal growth factor (Roche Diagnostics, Indianapolis, IN), and 1 ng/ml basic fibroblast growth factor (Roche Diagnostics) as described previously (Estes et al., 2006). Before mechanical testing, P4 ADAS cells were seeded onto PLL-coated Petri dishes for 1 h and 1 day and tested at room temperature in culture media.

2.1.5. Mesenchymal stem cells

MSCs harvested from normal human bone marrow were purchased from Cambrex (two donors) and the Tulane Center for Gene Therapy (one donor) ($n = 53$ spherical, $n = 67$ spread cells, ages: 28–34 years). Cells from each donor were expanded to P3 using Mesenchymal Stem Cell Medium (Cambrex) and then combined into a single “superlot” that was passaged once more to P4. MSCs were then seeded onto PLL-coated Petri dishes and tested at 1 h and 1 day in culture media.

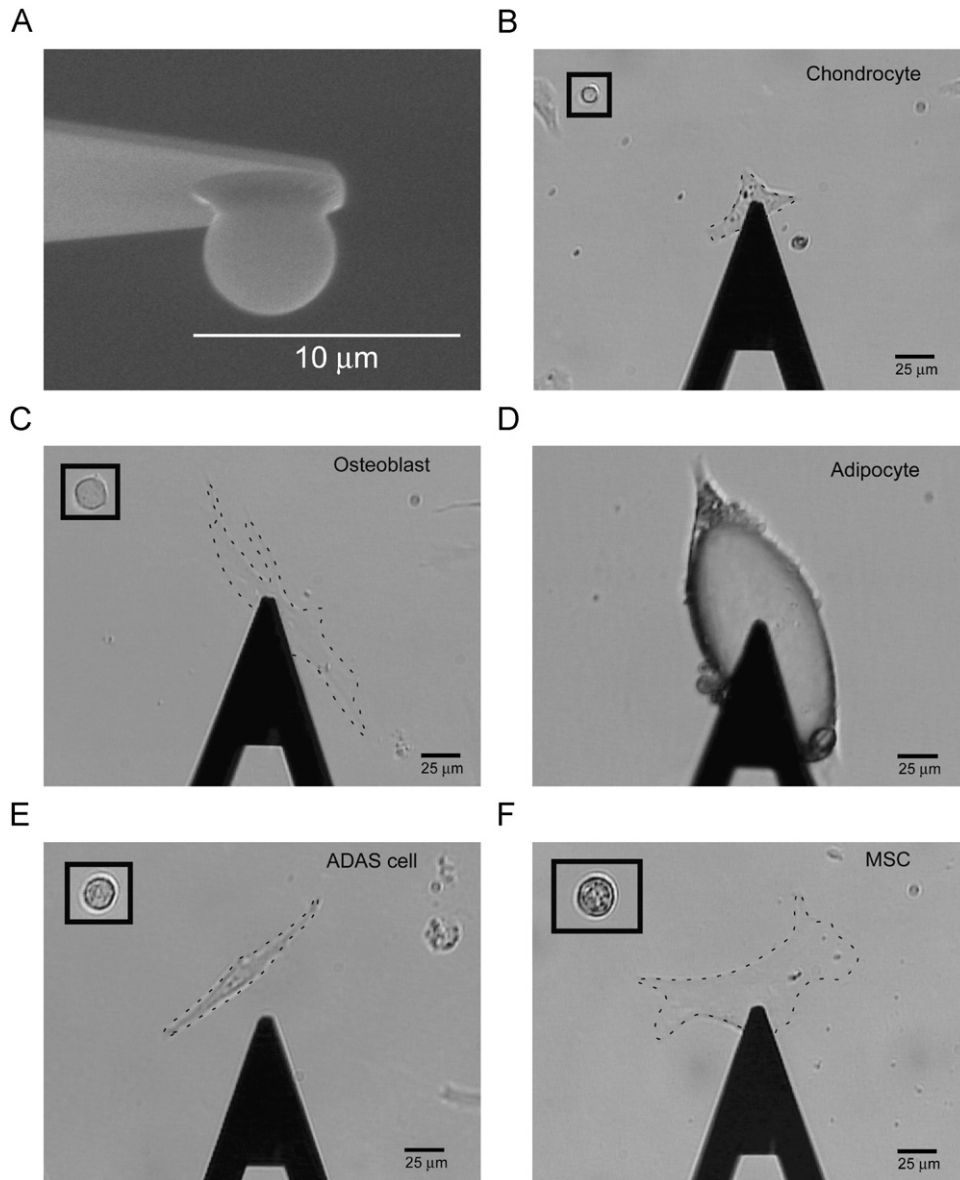


Fig. 1. **AFM indentation of single cells.** Indentation with a spherical-tip AFM probe (A) occurred at the center of the cell for the spherical morphology (inset pictures) and over the nucleus for the spread morphology. Polarized light images show a chondrocyte (B), osteoblast (C), adipocyte (D), ADAS cell (E), and MSC (F) highlighted by a dashed line surrounding their periphery.

2.2. Atomic force microscopy

The biomechanical properties of single cells were measured using an atomic force microscope (MFP-3D, Asylum Research, Santa Barbara, CA) via elastic and viscoelastic tests as described previously (Darling et al., 2006). Borosilicate glass spheres (5 μm diameter) were attached to the tip of AFM cantilevers ($k \sim 0.04$ N/m, Novascan Technologies, Inc., Ames, IA) used for stress relaxation experiments. Indentation was performed over the center of the nucleus (Fig. 1) at 15 μm/s, chosen to approximate a step displacement appropriate for the stress relaxation model. Elastic curves were sampled at 5 kHz, while viscoelastic curves were collected at 100–200 Hz for 60 s. A 2–3 nN force trigger was used to prescribe the point at which the cantilever approach was stopped and either retracted for elastic tests or held constant for viscoelastic tests. Linear drift in the laser was corrected for during data analysis.

The elastic modulus, E_{elastic} , was extracted from force vs. indentation data using an appropriate thin-layer Hertz model while E_{equil} values were

calculated using the force and indentation data at the end of the 60 s relaxation test. Probe-cell contact was identified using contact point extrapolation, a method that uses the indentation portion of the approach curve to determine where probe-cell contact begins (Guo and Akhremitchev, 2006) (see Appendix A). Stress relaxation tests were performed on the central region of cells for both spherical and spread morphologies. The parameters E_R , E_0 , μ , τ_σ , and τ_ϵ , were determined using a thin-layer, stress relaxation model of a viscoelastic solid (Darling et al., 2007). The Poisson's ratio (ν) for all cells was assumed to be 0.5, and parametric studies showed that varying ν from 0.3 to 0.5 altered the measured properties by less than 20%.

2.3. Statistical analysis

Data on cell mechanical properties were not normally distributed according to the Shapiro–Wilks test and were log-transformed before

statistical analysis. Two-factor ANOVA with Newman–Keuls post hoc analysis was performed using the Statistica software package (StatSoft, Tulsa, OK) to determine whether significant differences ($\alpha = 0.05$) in biomechanical properties existed among cell types and between morphologies. Biomechanical properties are reported as mean \pm standard deviation of the log-transformed data.

3. Results

3.1. Population distributions

Cell population properties were best described by log-normal distributions characterized by a shift towards lower moduli values. For spherical morphologies, osteoblasts, ADAS cells, and MSCs all exhibited broad distributions for E_{elastic} (Fig. 2). Chondrocytes and adipocytes had narrower ranges of elastic moduli with peaks at 1.1 and 0.61 kPa, respectively. For spread morphologies, E_{elastic} distributions did not change dramatically for any cell type except osteoblasts (Fig. 3), which showed an increase in the peak modulus from 2.0 kPa (spherical) to 5.8 kPa (spread). Other measured properties had similar distributions (see supplementary data, Figs. S3–S10).

3.2. Cell mechanical properties

Distinct biomechanical properties were observed among primary osteoblasts, chondrocytes, and adipocytes (Table 1). Elastic and viscoelastic fits were good ($R^2 = 0.9969$ and 0.7614 , respectively). Elastic properties varied significantly among cell types exhibiting spherical morphologies. For the primary cells, osteoblasts had the largest elastic moduli, followed by chondrocytes, then adipocytes ($p < 0.0002$). The adult stem cell populations exhibited similar E_{elastic} to each other and osteoblasts but were significantly larger than chondrocytes and adipocytes ($p < 0.0002$) (Fig. 4A). E_{equil} was similar for all cell types at short seeding times (see supplementary information, Fig. S1). Measured heights for spherical cells showed statistical differences for all cell type comparisons ($p < 0.0002$), except between chondrocytes and ADAS cells (Fig. 4B).

Viscoelastic properties for spherical cells did not show dramatic differences among the lineages tested. At short seeding times, osteoblasts, chondrocytes, and adipocytes all exhibited similar values for E_R (Fig. 5A). E_0 was lowest for chondrocytes and adipocytes ($p < 0.05$) (Fig. 5B), and μ

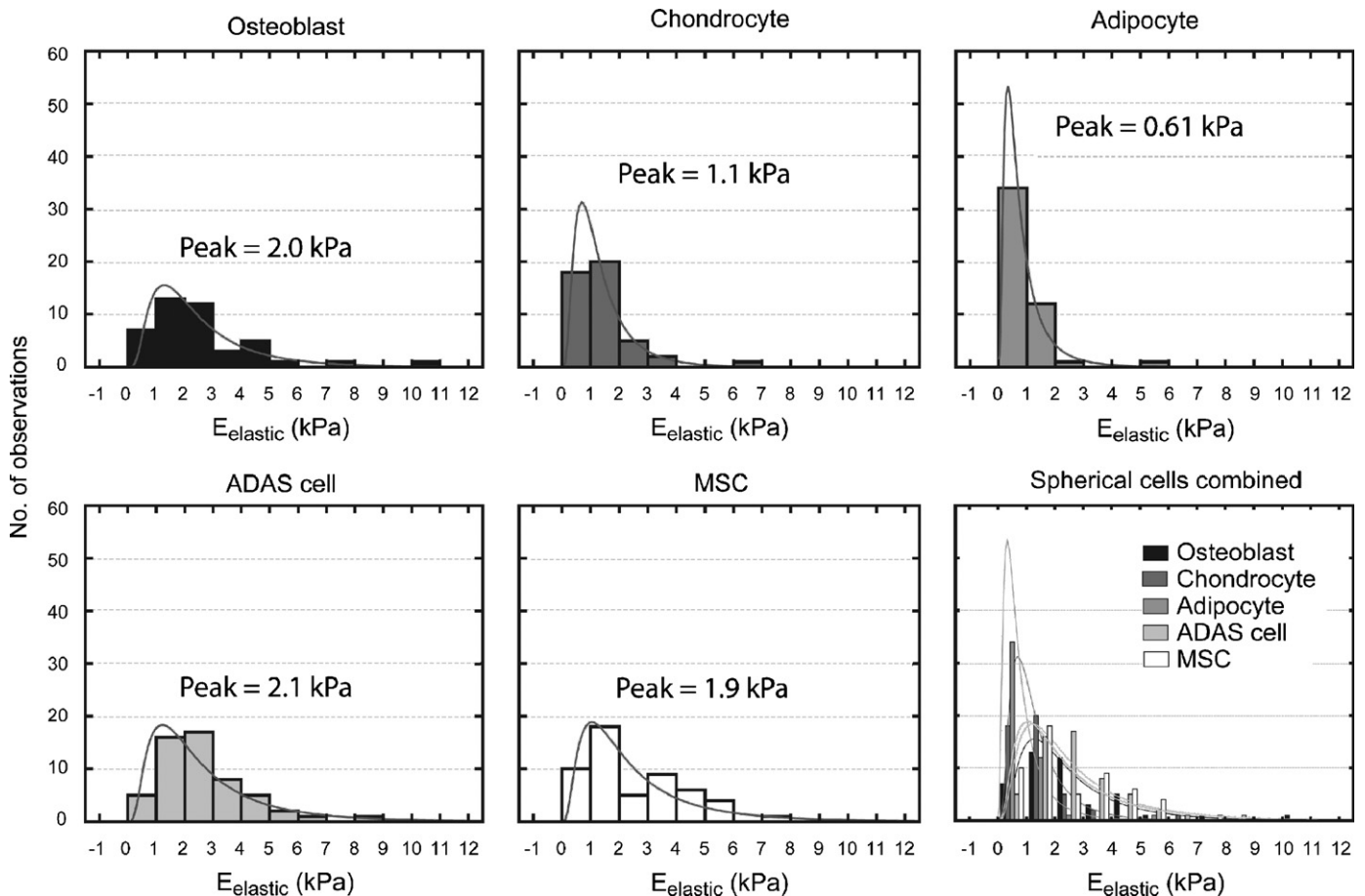


Fig. 2. E_{elastic} distribution for spherical cells. Elastic property distributions showed that osteoblasts, ADAS cells, and MSCs had similar variations within their populations. Chondrocytes and adipocytes had less variation and exhibited distribution peaks (lognormal fits) at lower elastic moduli than the other cell types.

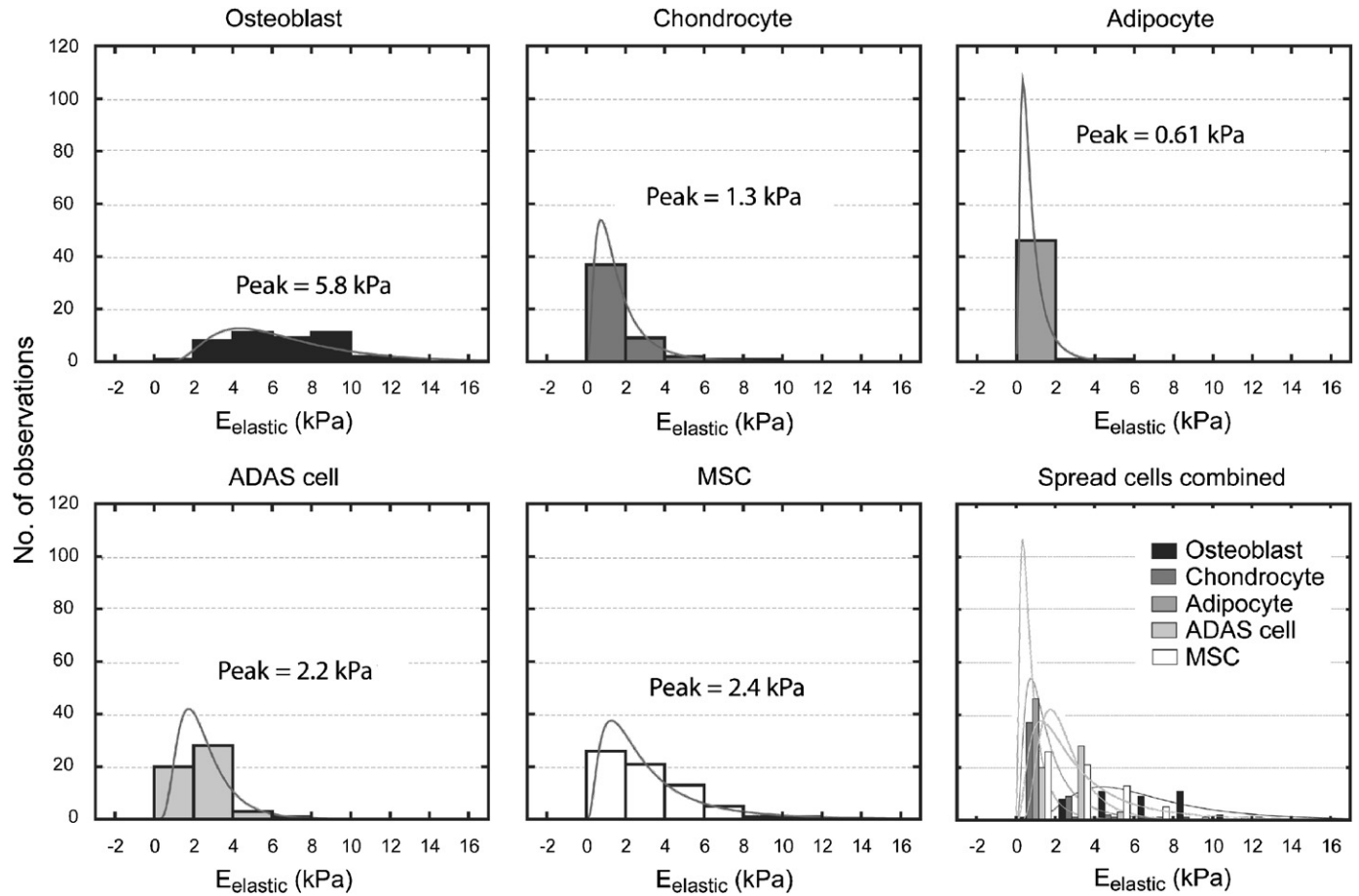


Fig. 3. E_{elastic} distribution for spread cells. Unlike the spherical morphology data, elastic properties for spread cells showed a distinct difference between osteoblasts and the other cell types. ADAS cells and MSCs exhibited similar population profiles, while chondrocytes did not change appreciably from their spherical morphology distributions. Adipocytes, which only exhibited one morphology, are shown for comparison purposes. Osteoblasts had the broadest distribution of elastic properties when spread, followed by MSCs then chondrocytes/ADAS cells.

Table 1
Elastic and viscoelastic fit parameters for osteoblasts, chondrocyte, adipocytes, ADAS cells, and MSCs in spherical and spread morphologies

	n	Elastic properties		Viscoelastic properties		
		E_{elastic} (kPa)	E_{equil} (kPa)	E_R (kPa)	τ_{σ} (s)	τ_{ϵ} (s)
Spherical						
Osteoblast	43	2.6 ± 2.0	0.60 ± 0.78	0.58 ± 0.68	24.6 ± 30.4	6.9 ± 3.3
Chondrocyte	46	1.4 ± 1.1	0.45 ± 0.42	0.45 ± 0.44	19.7 ± 15.6	9.7 ± 7.1
Adipocyte	48	0.9 ± 0.8	0.71 ± 0.74	0.61 ± 0.54	55.5 ± 129	31.1 ± 63.8
ADAS cell	55	2.6 ± 1.6	0.37 ± 0.31	0.37 ± 0.26	31.0 ± 41.5	7.3 ± 4.3
MSC	53	2.5 ± 1.8	0.52 ± 0.60	0.47 ± 0.52	108 ± 278	9.6 ± 11.3
Spread						
Osteoblast	43	6.5 ± 2.7	4.5 ± 2.3	4.3 ± 2.4	41.5 ± 101	15.4 ± 23.4
Chondrocyte	50	1.8 ± 1.7	1.0 ± 1.6	1.0 ± 1.6	14.1 ± 8.9	8.3 ± 5.5
ADAS cell	52	2.5 ± 1.2	1.7 ± 1.1	1.7 ± 1.0	21.5 ± 78.5	9.6 ± 16.0
MSC	67	3.2 ± 2.2	2.3 ± 2.1	2.2 ± 1.9	19.4 ± 55.3	10.1 ± 16.8

Data are presented as mean \pm standard deviation.

was statistically lower in adipocytes ($p < 0.005$) but displayed high variability in general (Fig. 5C). Adult stem cells also exhibited few differences in mechanical properties, although MSCs possessed a significantly lower value for E_R .

Under spread conditions, significant differences were observed in the biomechanical properties of primary cells. Elastic and viscoelastic models accurately fit the spread-cell data ($R^2 = 0.9949$ and 0.7665 , respectively) with the same quality as spherical morphology tests (see supplementary

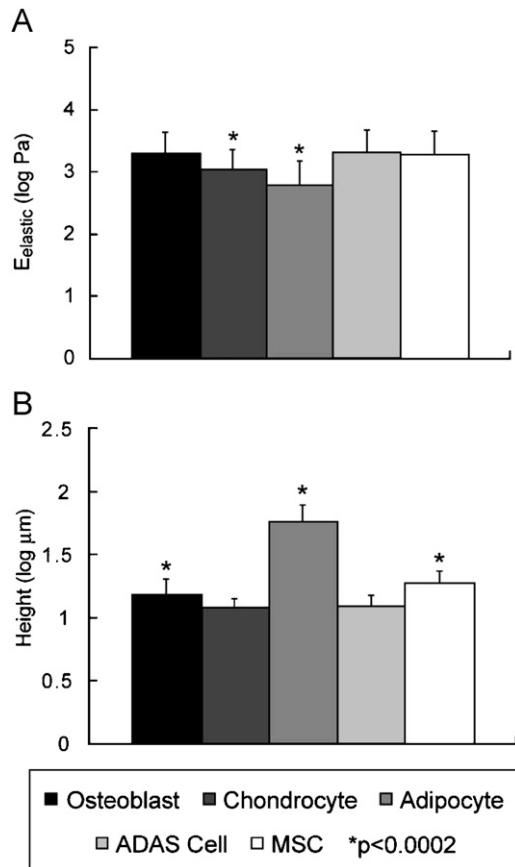


Fig. 4. E_{elastic} and height for spherical cells. Chondrocytes and adipocytes possessed E_{elastic} values that were significantly lower than the other cell types (A). Osteoblasts, ADAS cells, and MSCs all exhibited similar elastic properties when in a rounded cell shape. Cell heights were significantly different among all cell types, except between chondrocytes and ADAS cells (B). In particular, adipocytes were much larger than any of the other cell types. Data shown as mean \pm standard deviation of log-normalized values.

data, Fig. S2). In general, cells were stiffer when spread, although the magnitude of change depended on cell type. Osteoblasts showed the greatest increase in average moduli from spherical to spread, with a 1.5-fold increase in E_{elastic} ($p < 0.0001$) and a 6.5-fold increase in E_{R} ($p < 0.0001$). ADAS cells showed no significant change in E_{elastic} ($p = 0.98$) but a 3.5-fold increase in E_{R} ($p < 0.0001$). MSCs acted similarly, with no difference in E_{elastic} ($p = 0.23$) but a 3.7-fold increase in E_{R} ($p < 0.0001$).

Elastic properties for spread cells followed similar trends as those of spherical cells (Fig. 6A). For E_{equil} , osteoblasts were significantly stiffer than chondrocytes and adipocytes ($p < 0.0001$), but chondrocytes and adipocytes were not statistically different from each other ($p = 0.20$) (data not shown). Cell heights, however, were significantly different for all spread cell types ($p < 0.0001$) (Fig. 6B). Stem cells exhibited elastic properties intermediate between chondrocyte and osteoblast properties, with E_{elastic} and E_{equil} values being significantly higher than chondrocytes and adipocytes and significantly lower than osteoblasts ($p < 0.0001$).

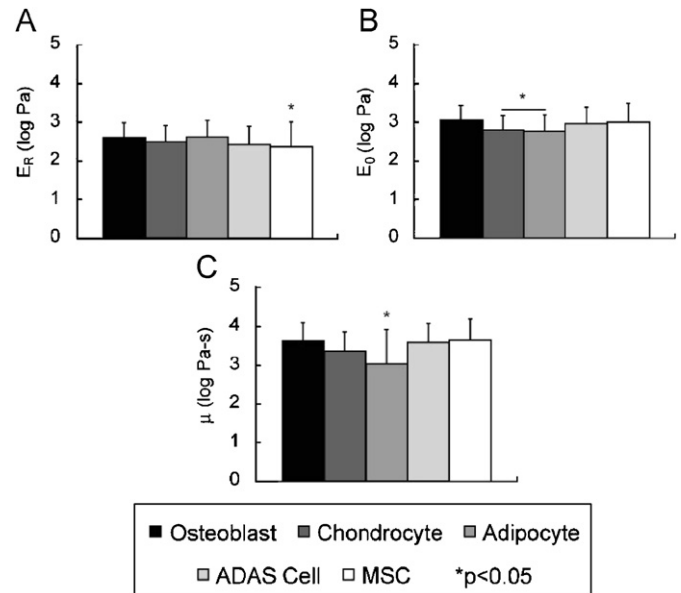


Fig. 5. E_{R} , E_0 , and μ for spherical cells. Few differences existed for E_{R} (A), E_0 (B), or μ (C) among cell types tested in the spherical morphology. This result could indicate that cellular viscoelastic characteristics are not apparent until a firm attachment to a surrounding matrix has been established. Data shown as mean \pm standard deviation of log-normalized values.

Significant differences were also present when comparing the viscoelastic properties of spread cell types (Fig. 7A–C). Osteoblasts exhibited higher E_{R} , E_0 , and μ than either chondrocytes or adipocytes ($p < 0.002$). Adipocytes possessed lower E_0 and μ values than other lineages ($p < 0.005$). However, no difference for E_{R} was observed between spread chondrocytes and adipocytes ($p = 0.12$). Stem cells had noticeably different properties from primary cell types. E_{R} and E_0 values for spread ADAS cells and MSCs were higher than that of chondrocytes and adipocytes but were lower than that of osteoblasts ($p < 0.0001$). The apparent viscosity of adult stem cells was lower than that of osteoblasts ($p < 0.0001$) and higher than that of adipocytes ($p < 0.0003$).

4. Discussion

The results of this study indicate that mechanical properties of cells may serve as biomarkers of their phenotype or tissue of origin. Notably, distinct differences were observed among primary cell types in comparison to either type of adult stem cell, indicating that cellular mechanical properties may provide an important marker of the differentiated state of a cell. An important finding of this study is the potential role of both elastic and viscoelastic properties in characterizing cell properties, which was most apparent in the ratio of E_{elastic} to E_{R} for spherical cells (Fig. 8). Both populations of adult stem cells exhibited significantly higher E_{elastic} to E_{R} ratios than primary cells ($p < 0.0001$). This relationship could thus be an important marker for the stem cell “phenotype”. A high

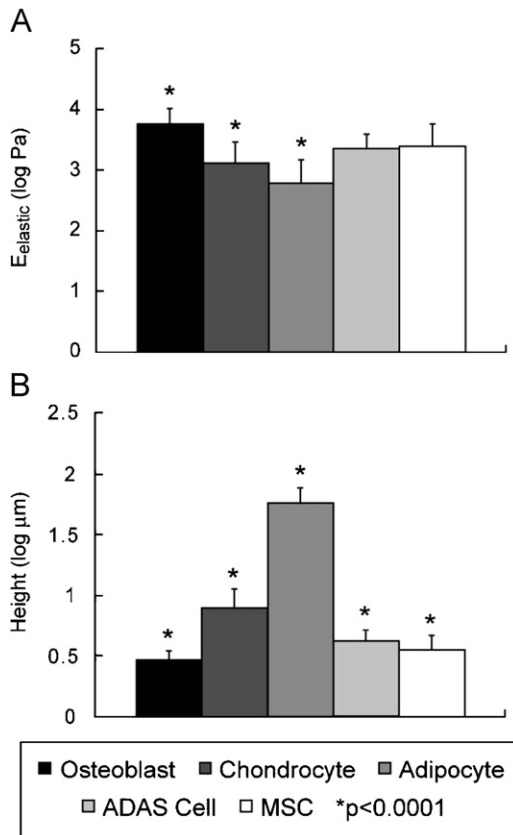


Fig. 6. E_{elastic} and height for spread cells. Elastic modulus varied significantly among cell types, with osteoblasts possessing the highest and adipocytes the lowest (A). Adult stem cells exhibited similar elastic properties that were intermediate between primary cell types. Cell heights indicated that osteoblasts, ADAS cells, and MSCs all spread to approximately the same height while chondrocytes remained much taller (B). Adipocytes, which were tested in just one morphology, are included for comparison purposes. Data shown as mean \pm standard deviation of log-normalized values.

ratio indicates that stem cells are initially very stiff upon loading but cannot sustain a resistance to load over time. A possible explanation for this response is the weak association between cell membrane and cytoskeleton in mesenchymal stem cells (Titushkin and Cho, 2006).

Cellular mechanical properties were not normally distributed, suggesting that subpopulations of cells with different properties exist within all tested groups. For example, the chondrocyte population is composed of superficial, middle, and deep zone cells, all of which exhibit different mechanical properties. Past studies have shown that middle/deep zone cells are less stiff than superficial zone cells but comprise a greater percentage of the total cell population (Darling et al., 2006) and could thus be responsible for the shift to lower moduli values for the overall property distributions observed here.

Cells were tested in two configurations: short seeding times provided a consistent testing morphology (spherical) for comparison among cell types, while longer seeding times (spread) helped determine whether differences were

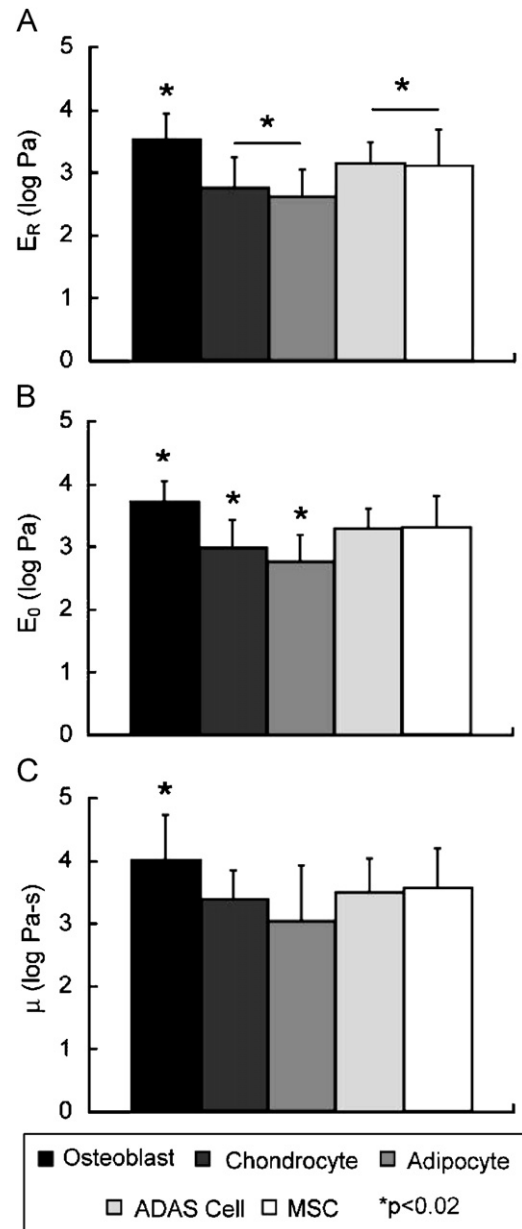


Fig. 7. E_R , E_0 , and μ for spread cells. Viscoelastic properties for the spread morphology showed significant differences for all comparisons of E_R except between chondrocytes and adipocytes and between ADAS cells and MSCs (A). All primary cell types were significantly different when comparing E_0 (B). The apparent viscosity of osteoblasts was significantly higher than all other cell types but exhibited extremely large variations, indicating that the preciseness of this property might not be sufficient for cell-to-cell comparisons (C). Data shown as mean \pm standard deviation of log-normalized values.

retained after an equilibrium shape was reached. No dramatic differences in viscoelastic properties were observed among cell lineages in a spherical morphology. Rounded cells and cells in suspension typically have a cortical shell of F-actin fibers, while spread cells have a variably stressed network of F-actin fibers that are attached to the substrate (Pritchard and Guilak, 2004). Thus the lack of differences among cell types may be due to

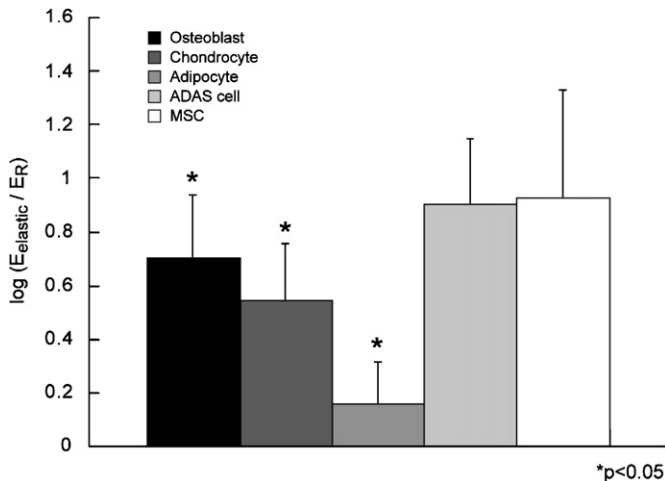


Fig. 8. E_{elastic}/E_R ratio for spherical cells. Adult stem cells exhibited a distinct trait when compared to primary cell types. Both ADAS cells and MSCs possessed high elastic moduli in comparison to their relaxed moduli. This result is shown most clearly by calculating a ratio of E_{elastic} to E_R . Physically, this value indicates that, in comparison to primary cells, stem cells are initially very stiff but cannot resist deformation due to load over time. Data shown as mean \pm standard deviation of log-normalized ratios.

the similar cytoskeletal architecture in this configuration. Differences among the lineages became apparent once the cells equilibrated in the spread morphology with anchored cytoskeletal structures. The cytoskeleton has been shown to play a major role in measured cell properties and is likely to be the main contributor in this study as cells polymerize an F-actin network in their spread morphologies (Pan et al., 2005; Trickey et al., 2004). Furthermore, recent studies suggest that human MSCs alter their F-actin structure during differentiation (Yourek et al., 2007).

Under most conditions, cell height was negatively correlated with cell moduli. To investigate the overall effect, adipocytes were omitted from the analysis, since their heights were on average three times that of the other cells. Larger heights correlated with lower moduli, apparent viscosity, and E_{elastic}/E_R ratios, accounting for 25–50% of the observed changes. As the theoretical model used in this study corrected for the thickness of the cell layer (Darling et al., 2006, 2007; Dimitriadis et al., 2002), this finding is likely due to other factors, such as the increased stiffness and organization of the F-actin cytoskeleton as cells spread (McGarry and Prendergast, 2004), or a larger contribution from the nucleus, which has been found to be 3–4 times stiffer than the cell as a whole (Guilak et al., 2000). However, in other studies that map the elastic modulus over the entire area of spread cells, we have observed that the elastic modulus varies minimally across the body of the cell (i.e., nucleus and peri-nuclear region) in comparison to the thinner edges, which exhibit much larger moduli (unpublished results). Taken together, these findings support the hypothesis that differences in

cell moduli and viscoelasticity are due to differences in cytoskeletal properties that are influenced by both differentiation state and local environment.

Our findings are generally consistent with previous reports of the mechanical properties of cells of mesenchymal origin, measured using a variety of techniques (reviewed in Table 2). While each technique has specific advantages and disadvantages, direct comparisons among methods are difficult due to the intrinsic assumptions involved in different testing methods. Past studies support the current finding that osteoblasts are intrinsically stiffer than chondrocytes. Fibroblasts, while not examined in this study, appear to have elastic moduli that are significantly lower than osteoblasts and slightly lower than chondrocytes for the spread morphology. Interestingly, chondrosarcoma cells, which are cancerous, mesenchymally derived cells that form a cartilaginous matrix, possess mechanical properties most similar to chondrocytes. While the two cell types likely do not experience a similar mechanical environment in vivo, they do reside in tissues with the same matrix composition (collagen and sulfated proteoglycans).

Although our findings are in general agreement with previous studies, some differences exist that may arise from variations in cell source, testing apparatus, and culture environment. Cells were harvested from several different species and anatomical locations, both of which could add significant variability to experiments. Testing method could also play a role. For example, AFM indentation tests occurred on cells adhered to an underlying substrate, which could affect the measured properties (Takai et al., 2005), while micropipette aspiration tests were applied to cells in suspension. Variability also exists among AFM experiments. However, this can be largely ascribed to the use of either spherical or pyramidal probe tips. Indentation experiments using sharp-tipped indenters typically result in higher measured moduli than those obtained with spherical-tipped indenters (Charras and Horton, 2002a, b). In some cases, mechanical property values may depend also on the choice of model used to derive the property from the measured data, in particular the assumption that a cell is either an elastic or viscoelastic material.

The results of this study pose an interesting question: Are cell mechanics intrinsic to a cell or are they only an acquired phenotype associated with its host tissue? Previous work has shown that MSC differentiation can be affected by matrix elasticity (Engler et al., 2006). For example, softer matrices that mimic neural tissue were neurogenic, whereas stiffer matrices that mimic bone were osteogenic. Since culture surface can influence not only differentiation but also apparent mechanical properties (Domke et al., 2000; Takai et al., 2005), the current study tested all cell types on the same material (PLL-coated polystyrene, with the exception of adipocytes which were on polystyrene). Results showed that cells had intrinsic biomechanical properties that were characteristic of their tissue of origin. A relationship between cell stiffness and

Table 2
Mechanical properties for a subset of mesenchymal lineage cells

Author, Year	Elastic/Young's modulus (kPa)	Cell source	Testing method	Notes
<i>Osteoblastic cells</i>				
Charras and Horton, (2002a)	14	Murine, neonatal long bones	AFM	Spread morphology on glass; pyramidal AFM tip
Charras and Horton, (2002b)	3.175	Murine, neonatal long bones	AFM	Spread morphology on glass; spherical AFM tip
Domke et al., (2000)	5.4–7.6	Human, SaOS2 osteoblast cell line	AFM	Spread morphology on glass/TCP; pyramidal AFM tip
Jaasma et al., (2006)	3–5 (converted to Hertz model)	Murine, MC3T3-E1 osteoblast cell line	AFM	Spread morphology on Col-I coated glass; spherical AFM tip
Shin and Athanasiou, (1999)	0.92–1.09	Human, MG63 osteosarcoma cell line	Cytoindentation	Spherical morphology on silicone, flat tip
Takai et al., (2005)	1.2	Murine, MC3T3-E1 osteoblast cell line	AFM	Spread morphology on PLL; pyramidal AFM tip
<i>Chondrocytes</i>				
Bader et al., (2002)	2.7	Bovine, adult cartilage	Compression of cell-seeded constructs	Spherical morphology, embedded in agarose
Darling et al., (2006)	0.6–1.2	Porcine, adult cartilage	AFM	Spherical morphology on PLL-coated glass; spherical AFM tip
Koay et al., (2003)	1.11	Bovine, adult cartilage	Creep indentation	Spherical morphology on glass
Leipzig and Athanasiou, (2005)	2.55	Bovine, adult cartilage	Unconfined creep compression	Spherical morphology on TCP
Shieh and Athanasiou, (2006)	1.17	Bovine, adult cartilage	Unconfined creep compression	Spherical morphology on glass
Trickey et al., (2000)	0.36	Human, adult cartilage	Micropipette aspiration	Spherical morphology
<i>Fibroblasts</i>				
Jaasma et al., (2006)	1–2 (converted to Hertz model)	Murine, NIH3T3 fibroblast cell line	AFM	Spread morphology on Col-I coated glass; spherical AFM tip
Mahaffy et al., (2000)	0.75–1.4	Murine, NIH3T3 fibroblast cell line	AFM	Spread morphology on glass; spherical AFM tip
Mahaffy et al., (2004)	0.6	Murine, NIH3T3 fibroblast cell line	AFM	Spread morphology on glass; spherical AFM tip
Petersen et al., (1982)	4–14	Murine, 3T3 fibroblast cell line	cell poker	Spread morphology on glass; spherical-tipped poker
Wu et al., (1998)	4	Murine, L929 fibroblast cell line	AFM	Spread morphology on TCP; pyramidal AFM tip
Thoumine and Ott, (1997)	14.7	Avian, heart fibroblasts	Microplate compression	Spherical morphology; glass plates
<i>Mesenchymal stem cells</i>				
Pan et al., (2005)	0.56	Human, bone marrow	Micropipette aspiration	Spherical morphology
Yourek et al., (2007)	33	Human, bone marrow	AFM	Spread morphology on TCP; pyramidal AFM tip, spherical Hertz model
<i>Chondrosarcoma cells</i>				
Darling et al., (2007)	1–2.5	Human, 3 different chondrosarcoma cell lines	AFM	Spherical/spread morphologies on PLL/TCP; spherical AFM tip

Results show large variations among studies, due primarily to the different mechanical models, cell lines, and testing methods employed. When applicable, apparent moduli values were converted by assuming $\nu = 0.5$ (PLL: poly-L-lysine; TCP: tissue culture plastic)

tissue stiffness exists for the primary cells, with osteoblasts/bone being stiffer than chondrocytes/cartilage, which in turn were stiffer than adipocytes/fat. A correlation was not observed, however, for stem cells, which may reflect their undifferentiated state.

Our findings indicate that primary cells and stem cells possess characteristic mechanical biomarkers that are present after isolation from native tissue. The ability to distinguish cells in a lineage-specific manner may thus

provide a method for sorting or enriching heterogeneous populations of adult stem cells, although the application of such approaches will require the development of new, higher-throughput methods for mechanical testing of cells. Current, biochemically -based sorting procedures have had little success in producing multipotent populations from MSC harvests (Kolf et al., 2007). Furthermore, the biomechanical characterization of single osteoblasts, chondrocytes, adipocytes, ADAS cells, and MSCs may help to

more accurately model the mechanical microenvironment in musculoskeletal tissues.

Conflicts of interest

None of the authors have a conflict of interest associated with this work.

Acknowledgments

This work was supported in part by NIH Grants AR53448, EB01630, AG15768, AR48182, and AR50245. MSCs used in this study were provided by the Tulane Center for Gene Therapy through NIH grant P40RR0-17447. The authors would also like to thank Drs. Bill Whitlatch and Sam Adams for their contributions.

Appendix A. Supplementary data

Supplementary data associated with this article can be found in the online version at [doi:10.1016/j.jbiomech.2007.06.019](https://doi.org/10.1016/j.jbiomech.2007.06.019)

References

- Alexopoulos, L.G., Setton, L.A., Guilak, F., 2005. The biomechanical role of the chondrocyte pericellular matrix in articular cartilage. *Acta Biomaterialia* 1, 317–325.
- Bader, D.L., Ohashi, T., Knight, M.M., Lee, D.A., Sato, M., 2002. Deformation properties of articular chondrocytes: a critique of three separate techniques. *Biorheology* 39, 69–78.
- Bausch, A.R., Ziemann, F., Boulbitch, A.A., Jacobson, K., Sackmann, E., 1998. Local measurements of viscoelastic parameters of adherent cell surfaces by magnetic bead microrheometry. *Biophysical Journal* 75, 2038–2049.
- Buckwalter, J.A., Martin, J.A., Brown, T.D., 2006. Perspectives on chondrocyte mechanobiology and osteoarthritis. *Biorheology* 43, 603–609.
- Burkholder, T.J., 2007. Mechanotransduction in skeletal muscle. *Frontiers in Bioscience* 12, 174–191.
- Caplan, A.L., 1991. Mesenchymal stem cells. *Journal of Orthopaedic Research* 9, 641–650.
- Charras, G.T., Horton, M.A., 2002a. Determination of cellular strains by combined atomic force microscopy and finite element modeling. *Biophysical Journal* 83, 858–879.
- Charras, G.T., Horton, M.A., 2002b. Single cell mechanotransduction and its modulation analyzed by atomic force microscope indentation. *Biophysical Journal* 82, 2970–2981.
- Costa, K.D., 2003. Single-cell elastography: probing for disease with the atomic force microscope. *Disease Markers* 19, 139–154.
- Darling, E.M., Zauscher, S., Block, J.A., Guilak, F., 2007. A thin-layer model for viscoelastic, stress-relaxation testing of cells using atomic force microscopy: do cell properties reflect metastatic potential? *Biophysical Journal* 92, 1784–1791.
- Darling, E.M., Zauscher, S., Guilak, F., 2006. Viscoelastic properties of zonal articular chondrocytes measured by atomic force microscopy. *Osteoarthritis and Cartilage* 14, 571–579.
- Dimitriadis, E.K., Horkay, F., Maresca, J., Kachar, B., Chadwick, R.S., 2002. Determination of elastic moduli of thin layers of soft material using the atomic force microscope. *Biophysical Journal* 82, 2798–2810.
- Domke, J., Dannohl, S., Parak, W.J., Muller, O., Aicher, W.K., Radmacher, M., 2000. Substrate dependent differences in morphology and elasticity of living osteoblasts investigated by atomic force microscopy. *Colloids and Surfaces B—Biointerfaces* 19, 367–379.
- Engler, A.J., Sen, S., Sweeney, H.L., Discher, D.E., 2006. Matrix elasticity directs stem cell lineage specification. *Cell* 126, 677–689.
- Estes, B.T., Wu, A.W., Storms, R.W., Guilak, F., 2006. Extended passaging, but not aldehyde dehydrogenase activity, increases the chondrogenic potential of human adipose-derived adult stem cells. *Journal of Cellular Physiology* 209, 987–995.
- Evans, E., Yeung, A., 1989. Apparent viscosity and cortical tension of blood granulocytes determined by micropipet aspiration. *Biophysical Journal* 56, 151–160.
- Fermor, B., Gundle, R., Evans, M., Emerton, M., Pocock, A., Murray, D., 1998. Primary human osteoblast proliferation and prostaglandin E2 release in response to mechanical strain in vitro. *Bone* 22, 637–643.
- Fernyhough, M.E., Vierck, J.L., Hausman, G.J., Mir, P.S., Okine, E.K., Dodson, M.V., 2004. Primary adipocyte culture: Adipocyte purification methods may lead to a new understanding of adipose tissue growth and development. *Cytotechnology* 46, 163–172.
- Gimble, J.M., Guilak, F., 2003. Differentiation potential of adipose derived adult stem (ADAS) cells. *Current Topics in Developmental Biology* 58, 137–160.
- Guck, J., Schinkinger, S., Lincoln, B., Wottawah, F., Ebert, S., Romeyke, M., Lenz, D., Erickson, H.M., Ananthakrishnan, R., Mitchell, D., Kas, J., Ulvick, S., Bilby, C., 2005. Optical deformability as an inherent cell marker for testing malignant transformation and metastatic competence. *Biophysical Journal* 88, 3689–3698.
- Guilak, F., 2000. The deformation behavior and viscoelastic properties of chondrocytes in articular cartilage. *Biorheology* 37, 27–44.
- Guilak, F., Lott, K.E., Awad, H.A., Cao, Q., Hicok, K.C., Fermor, B., Gimble, J.M., 2006. Clonal analysis of the differentiation potential of human adipose-derived adult stem cells. *Journal of Cellular Physiology* 206, 229–237.
- Guilak, F., Mow, V.C., 2000. The mechanical environment of the chondrocyte: a biphasic finite element model of cell–matrix interactions in articular cartilage. *Journal of Biomechanics* 33, 1663–1673.
- Guilak, F., Sah, R.L., Setton, L.A., 1997. Physical regulation of cartilage metabolism. In: Mow, V.C., Hayes, W.C. (Eds.), *Basic Orthopaedic Biomechanics*. Lippincott-Raven, Philadelphia, pp. 179–207.
- Guilak, F., Tedrow, J.R., Burgkart, R., 2000. Viscoelastic properties of the cell nucleus. *Biochemical and Biophysical Research Communications* 269, 781–786.
- Gundle, R., Beresford, J.N., 1995. The isolation and culture of cells from explants of human trabecular bone. *Calcified Tissue International* 56 (Suppl. 1), S8–S10.
- Gundle, R., Joyner, C.J., Triffitt, J.T., 1995. Human bone tissue formation in diffusion chamber culture in vivo by bone-derived cells and marrow stromal fibroblastic cells. *Bone* 16, 597–601.
- Guo, S., Akhremitchev, B.B., 2006. Packing density and structural heterogeneity of insulin amyloid fibrils measured by AFM nanoindentation. *Biomacromolecules* 7, 1630–1636.
- Hochmuth, R.M., 2000. Micropipette aspiration of living cells. *Journal of Biomechanics* 33, 15–22.
- Huang, H., Kamm, R.D., Lee, R.T., 2004. Cell mechanics and mechanotransduction: pathways, probes, and physiology. *American Journal of Physiology—Cell Physiology* 287, C1–C11.
- Ingber, D.E., 2003. Mechanobiology and diseases of mechanotransduction. *Annals of Medicine* 35, 564–577.
- Ingber, D.E., 2006. Cellular mechanotransduction: putting all the pieces together again. *FASEB Journal* 20, 811–827.
- Jaasma, M.J., Jackson, W.M., Keaveny, T.M., 2006. The effects of morphology, confluency, and phenotype on whole-cell mechanical behavior. *Annals of Biomedical Engineering* 34, 759–768.
- Jiang, Y., Jahagirdar, B.N., Reinhardt, R.L., Schwartz, R.E., Keene, C.D., Ortiz-Gonzalez, X.R., Reyes, M., Lenvik, T., Lund, T., Blackstad, M., Du, J., Aldrich, S., Lisberg, A., Low, W.C., Largaespada, D.A., Verfaillie, C.M., 2002. Pluripotency of mesenchymal stem cells derived from adult marrow. *Nature* 418, 41–49.

- Koay, E.J., Shieh, A.C., Athanasiou, K.A., 2003. Creep indentation of single cells. *Journal of Biomechanical Engineering* 125, 334–341.
- Kolf, C.M., Cho, E., Tuan, R.S., 2007. Mesenchymal stromal cells. Biology of adult mesenchymal stem cells: regulation of niche, self-renewal and differentiation. *Arthritis Research and Therapy* 9, 204.
- Kuettner, K.E., Pauli, B.U., Gall, G., Memoli, V.A., Schenk, R.K., 1982. Synthesis of cartilage matrix by mammalian chondrocytes in vitro. I. Isolation, culture characteristics, and morphology. *Journal of Cell Biology* 93, 743–750.
- Leipzig, N.D., Athanasiou, K.A., 2005. Unconfined creep compression of chondrocytes. *Journal of Biomechanics* 38, 77–85.
- Liedert, A., Kaspar, D., Blakytyn, R., Claes, L., Ignatius, A., 2006. Signal transduction pathways involved in mechanotransduction in bone cells. *Biochemical and Biophysical Research Communications* 349, 1–5.
- Mahaffy, R.E., Park, S., Gerde, E., Kas, J., Shih, C.K., 2004. Quantitative analysis of the viscoelastic properties of thin regions of fibroblasts using atomic force microscopy. *Biophysical Journal* 86, 1777–1793.
- Mahaffy, R.E., Shih, C.K., MacKintosh, F.C., Kas, J., 2000. Scanning probe-based frequency-dependent microrheology of polymer gels and biological cells. *Physical Review Letters* 85, 880–883.
- McGarry, J.G., Prendergast, P.J., 2004. A three-dimensional finite element model of an adherent eukaryotic cell. *European Cells and Materials* 7, 27–33 (discussion 33–24).
- Ng, A.M., Saim, A.B., Tan, K.K., Tan, G.H., Mokhtar, S.A., Rose, I.M., Othman, F., Idrus, R.B., 2005. Comparison of bioengineered human bone construct from four sources of osteogenic cells. *Journal of Orthopaedic Science* 10, 192–199.
- Pan, W., Petersen, E., Cai, N., Ma, G., Run Lee, J., Feng, Z., Liao, K., Leong, K., 2005. Viscoelastic properties of human mesenchymal stem cells. In: conference Proceedings of IEEE Engineering in Medicine and Biology Society 5, 4854–4857.
- Petersen, N.O., McConnaughey, W.B., Elson, E.L., 1982. Dependence of locally measured cellular deformability on position on the cell, temperature, and cytochalasin B. *Proceedings of the National Academy of Sciences of the United States of America* 79, 5327–5331.
- Pritchard, S., Guilak, F., 2004. The role of F-actin in hypo-osmotically induced cell volume change and calcium signaling in anulus fibrosus cells. *Annals of Biomedical Engineering* 32, 103–111.
- Robling, A.G., Castillo, A.B., Turner, C.H., 2006. Biomechanical and molecular regulation of bone remodeling. *Annual Review of Biomedical Engineering* 8, 455–498.
- Setton, L.A., Chen, J., 2004. Cell mechanics and mechanobiology in the intervertebral disc. *Spine* 29, 2710–2723.
- Shieh, A.C., Athanasiou, K.A., 2006. Biomechanics of single zonal chondrocytes. *Journal of Biomechanics* 39, 1595–1602.
- Shin, D., Athanasiou, K., 1999. Cytoindentation for obtaining cell biomechanical properties. *Journal of Orthopaedic Research* 17, 880–890.
- Takai, E., Costa, K.D., Shaheen, A., Hung, C.T., Guo, X.E., 2005. Osteoblast elastic modulus measured by atomic force microscopy is substrate dependent. *Annals of Biomedical Engineering* 33, 963–971.
- Thoumine, O., Ott, A., 1997. Comparison of the mechanical properties of normal and transformed fibroblasts. *Biorheology* 34, 309–326.
- Titushkin, I., Cho, M., 2006. Distinct membrane mechanical properties of human mesenchymal stem cells determined using laser optical tweezers. *Biophysical Journal* 90, 2582–2591.
- Trickey, W.R., Lee, G.M., Guilak, F., 2000. Viscoelastic properties of chondrocytes from normal and osteoarthritic human cartilage. *Journal of Orthopaedic Research* 18, 891–898.
- Trickey, W.R., Vail, T.P., Guilak, F., 2004. The role of the cytoskeleton in the viscoelastic properties of human articular chondrocytes. *Journal of Orthopaedic Research* 22, 131–139.
- Wu, H.W., Kuhn, T., Moy, V.T., 1998. Mechanical properties of L929 cells measured by atomic force microscopy: effects of anti-cytoskeletal drugs and membrane crosslinking. *Scanning* 20, 389–397.
- Yourek, G., Hussain, M.A., Mao, J.J., 2007. Cytoskeletal changes of mesenchymal stem cells during differentiation. *ASAIO Journal* 53, 219–228.
- Zhang, H.H., Kumar, S., Barnett, A.H., Eggo, M.C., 2000. Ceiling culture of mature human adipocytes: use in studies of adipocyte functions. *Journal of Endocrinology* 164, 119–128.
- Zhu, C., Bao, G., Wang, N., 2000. Cell mechanics: mechanical response, cell adhesion, and molecular deformation. *Annual Review of Biomedical Engineering* 2, 189–226.